Preparation and Electrochemical Performance of Polycrystalline and Single Crystalline CuO Nanorods as Anode Materials for Li Ion Battery

X. P. Gao,*,† J. L. Bao,† G. L. Pan,‡ H. Y. Zhu,*,§ P. X. Huang,† F. Wu,†,|| and D. Y. Song†

Institute of New Energy Chemistry Material, Nankai University, Tianjin 300071, China, State Key Laboratory of Functional Polymer Materials for Adsorption and Separation, Nankai University, Tianjin 300071, China, Electron Microscope Unit and School of Chemistry, The University of Sydney, NSW 2006, Australia, and School of Chemical Engineering and Environmental, Beijing Institute of Technology, Beijing 100081, China

Received: October 10, 2003; In Final Form: March 5, 2004

A simple and efficient approach is developed for the synthesis of copper oxide nanorods with different morphology and crystallographic structure. Polycrystalline fine rods 10−20 nm thick and several hundred nanometers long and single crystalline thick rods 60−100 nm thick and up to 1 μm long were obtained from the reactions of copper hydrate with caustic soda solution at room temperature and 100 °C, respectively. The fine CuO nanorods as anode materials for Li ion battery exhibit a high electrochemical capacity of 766 mA h/g and relatively poor capacity retention as compared to thick nanorods with the single crystalline structure. The correlation between the structural features of the nanorods and their electrode performance is discussed in detail.

I. Introduction

The pioneering work in carbon nanotubes has stimulated profound research interest worldwide in synthesizing nanoscale materials of various metals, polymers, metal oxides, and sulfides because of superior properties and potential applications of the new nanostructures.[1,2] In particular, the synthesis of inorganic nanomaterials with a regular morphology on a nanometer scale, such as nanotubes and nanorods, is of pronounced significance to material science. Copper oxide with nanometer-scale dimension and morphological specificity is an advanced material with potential for diverse applications as semiconductors, organic catalysts, gas sensors,[3] and lithium ion electrode materials.[4] Various methods for preparing copper oxide thin film, nanoparticles, and nanorods have been reported, such as electrochemical synthesis,[5] solid-state reactions,[6] a template method using carbon nanotubes[7] and thermal oxidation of copper substrates in air[8] or preparation with poly(ethylene glycol) (PEG) surfactant.[9] It is believed that the copper oxide rods formed in the presence of PEG surfactant through a surfactant assemblage because PEG in water can form a chain structure.[9,10] In addition, the nanostructured oxides of 3d transition metal elements exhibit reversible capacities 2−3 times larger than those of graphite as negative electrode materials for lithium ion batteries.[11] It has been identified that the size of the precursor particles has a crucial effect on the electrochemical behavior of these metal oxides toward lithium.[12] Here we report a novel and simple approach for the synthesis of copper oxide nanorods, without any surfactant or template. This approach has a bright perspective for large-scale and controllable production of copper oxide nanorods with various morphologies and crystallographic structures in large scales. The fine and bulk nanorods of CuO polycrystalline and single crystalline structure were prepared in alkaline solution at room temperature and 100 °C, respectively. The electrochemical reaction of lithium with the obtained CuO nanorods was investigated by cyclic voltammetry and galvanostatic method.

II. Experimental Section

Sample Preparation and Characterization. Copper hydroxide precipitates were prepared from a 0.5 M solution of NaOH and a 0.5 M solution of $CuCl_2$. The obtained precipitates were then dispersed in a 15 M solution of NaOH, and the dispersion was transferred into an autoclave with a PTFE container and kept at room temperature and 100 °C for 48 h, respectively. The precipitates were recovered from the autoclaved mixture and rinsed with distilled water until the pH approached about 7. The wet-cake samples were dried at 100 °C in air for 1 day. The morphology and crystal structure surface of the copper oxide nanorods were characterized using a transmission electron microscope (TEM, FEI Tecnai 20) with an accelerating voltage of 200 kV, and an X-ray diffractometer (XRD, Rigaku D/max-2500) with Cu Kα radiation. The infrared spectra of the nanorods were recorded on a Nicolet 5ZDX Fourier transform spectrometer in the spectra range of 4000−400 cm^{-1}, and CuO powder obtained from the decomposition of $Cu(OH)_2$ at 500 °C in air was used as a reference for blank baseline correction. Thermogravimetric analysis (TGA) was conducted on a NETZSCH TG 209 to monitor the mass loss of adsorbed water; specimens were heated at a heating rate of 10 deg/min and in a nitrogen gas flow.

Electrochemical Reaction of Li with CuO Nanorods. The working electrode was prepared by pressing a mixture of the active materials, conductive material (acetylene black), and binder (PTFE) in a weight ratio of 85/10/5. Lithium metal was used as the counter and reference electrodes. The electrolyte was 1 M $LiPF_6$ in a mixture of ethylene carbonate (EC), propylene carbonate (PC), and dimethyl carbonate (DMC). The

* Corresponding authors. X.P.G.: telephone, +86-22-23500876; fax, +86-22-23505371; e-mail, xpgao@nankai.edu.cn. H.Y.Z.: fax, 61 2 9351 7682; e-mail, h.zhu@emu.usyd.edu.au.

† Institute of New Energy Chemistry Material, Nankai University.

‡ State Key Laboratory of Functional Polymer Materials for Adsorption and Separation, Nankai University.

§ The University of Sydney.

|| Beijing Institute of Technology.

10.1021/jp037075k CCC: $27.50
Published on Web 04/10/2004

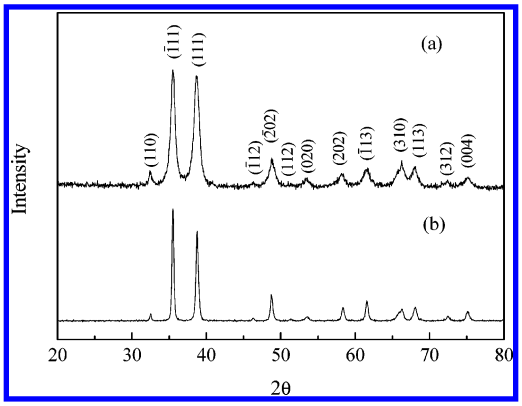

Figure 1. XRD patterns of as-prepared nanorods at room temperature (a) and 100 °C (b).

volume ratio of EC:PC:DMC in the mixture was 6:3:1. The galvanostatic method at the discharge−charge current density of 50 mA/g was used to measure the electrochemical capacity of the electrode at room temperature. The cyclic voltammetry (CV) experiment was carried out at the scan rate of 0.1 mV/s using a CHI 600A potentiostat at room temperature.

III. Results and Discussion

The XRD patterns of the samples as prepared at room temperature and 100 °C are shown in Figure 1. All peaks in the patterns of two samples are consistent with the JCPDS (5-0661) data of the copper oxide with a monoclinic phase.[13] This indicates that CuO can form even at room temperature when copper hydroxide precipitates are treated with a concentrated NaOH solution. However, the diffraction peaks of the sample obtained at room temperature are obviously broader than those for the sample prepared at 100 °C, suggesting that the former consists of much finer crystallites. The average crystalline sizes in the copper oxide samples at room temperature and 100 °C are estimated, using the Sherrer equation from the XRD patterns, to be 17 and 73 nm, respectively.

Hydrothermal treatments were shown to influence greatly the form of the copper oxide nanorods. The morphological features of the nanorods are highly dependent upon the temperature of the treatment with caustic soda in autoclaves during the synthesis. The product from treatment at room temperature was uniform fine nanorods about 10−20 nm thick and several hundred nanometers long (as shown in Figure 2), which are even thinner than the precursor of $Cu(OH)_2$ precipitates that are irregular particles of 40−60 nm in size. These fine nanorods tend to aggregate in spindle-like bundles because of their high surface energy or van der Waals forces, and this is similar to the bundles of single wall carbon nanotubes.[14] In contrast, bulk copper oxide nanorods were obtained at 100 °C, which have diameters of ca. 60−100 nm and lengths of up to 1.0 μm. Obviously the temperature of the treatment in autoclaves has a profound influence on the morphology and size of copper oxide nanomaterials. The selected area electron diffraction (SAED) patterns inserted in Figure 2 indicate an interesting fact that the bulk nanorods obtained at 100 °C consist of single crystals while the fine nanorods obtained at room temperature have a polycrystalline structure, although they both have monoclinic phase structure according to their XRD patterns. Raising the temperature of the hydrothermal treatment results in structure transformation of CuO nanorods from polycrystalline to single crystalline. This transformation may undergo the Ostwald ripening process in which larger crystallites grow at the expense

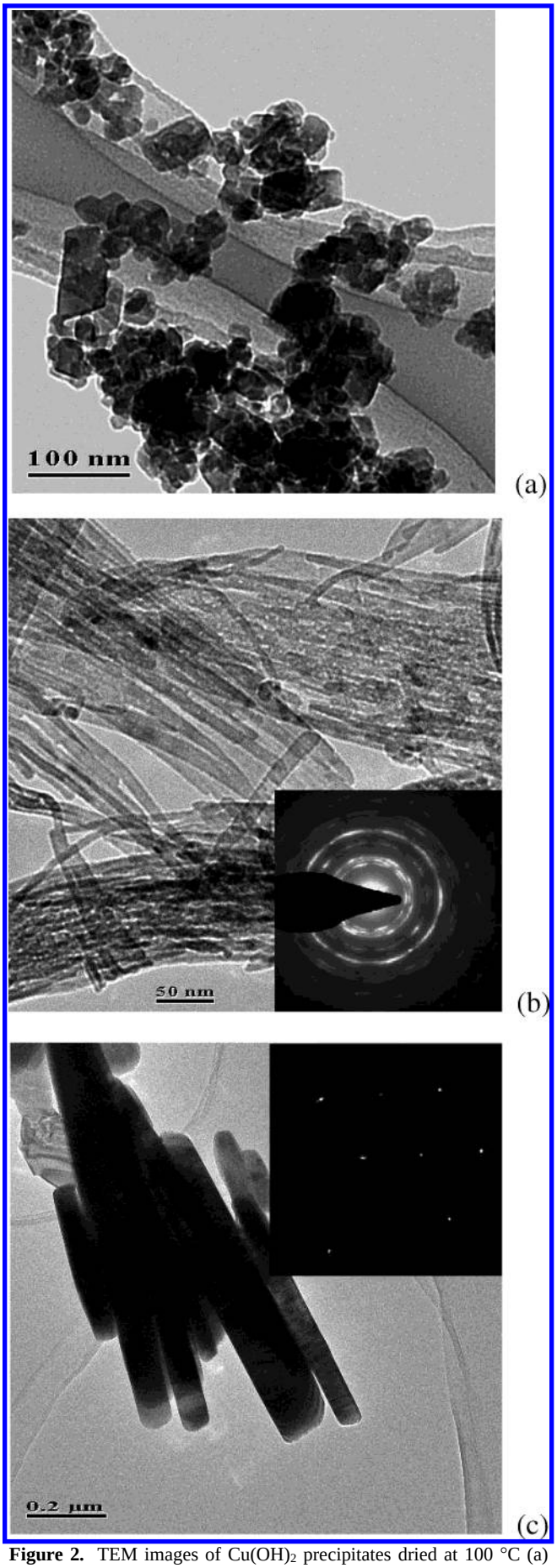

Figure 2. TEM images of $Cu(OH)_2$ precipitates dried at 100 °C (a) and as-prepared nanorods at room temperature (b) and 100 °C (c). The selected area electron diffraction of the as-prepared nanorods is inserted.

of smaller crystallites being dissolved.[15] Meanwhile, the spindle-like bundles of copper oxide nanorods grow into bulk nanorods or nanoplatelets as the temperature is raised.

It has been reported that TiO_2 or titanate nanotubes, nanorods, and nanoribbons can be synthesized hydrothermally in NaOH solution.[16−19] For both CuO and TiO_2 or titanate, one-dimensional nanostructures can be formed in concentrated NaOH solution under hydrothermal conditions without any surfactant and template. This suggests that these syntheses may follow a common mechanism, which could also be applied to other transition metal oxides. The difference is that TiO_2 or titanate nanotube and nanorods prepared from concentrated NaOH solution contain a large amount of crystal water,[16,19] while CuO nanorods prepared in NaOH solution contain no crystal water due to dehydration in the same solution. It was also found that, in a reaction solution of a high OH^- concentration, $Zn(OH)_4^{2-}$ precursor plays an important role in determining the morphologies of ZnO crystallites. The OH^- concentration in the reaction solution should be a key factor for controlling the growth rate of different crystal faces and thus lead to the formation of an anisotropic particle such as rod-like morphology as found in the preparation of ZnO nanorods.[20] However, $Cu(OH)_2$ precipitates cannot dissolve in concentrated NaOH solution to form dissoluble complex ions such as $Zn(OH)_4^{2-}$. Therefore, we believe that CuO crystalline nuclei of nanoscale size form during the dehydration process of $Cu(OH)_2$ precipitates in concentrated NaOH solution and grow gradually in a one-dimensional direction to result in the rod-like structure. The hydrothermal synthesis in NaOH solution is a simple and efficient method for producing various inorganic metallic oxide nanomaterials with a regular geometry and crystal structure.

Cyclic voltammograms (CVs) of electrodes made by fine and bulk nanorods at a scan rate of 0.1 mV/s are depicted in Figure 3. In the first cycle, the three cathodic peaks of lithium in the fine nanorod electrode are observed at 1.86, 1.05, and 0.74 V vs Li^+/Li in the voltammograms, respectively, corresponding to the multistep electrochemical lithium reaction process or additional sites for lithium intercalation. Meanwhile, only one main anodic peak is located near 2.51 V vs Li^+/Li, and a small shoulder is observed, corresponding to Li extraction from the crystal lattice of CuO.[21] In the second cycle, decreases of individual peak intensity and integral area, resulting in reversible capacity losses, are observed with shifts to 2.25, 1.23, and 0.78 V of the peak potentials in the cathodic direction. The change of peak potentials in CVs is in agreement with potential range in discharge curves as found in the next section. In the following cycles, there is no substantial change in the peak potentials and curve shape, which remain similar to those in the second cycle. In contrast, the main potential peaked at 1.08 V with two small shoulder peak potentials of 1.64 and 0.80 V for the bulk nanorod electrode in the first cycle, different from that of the fine nanorod electrode. This is obviously different from the voltammograms of the fine nanorod electrode. The substantial changes in main peak intensity and integral area of the bulk nanorod electrode in the second cycle indicate larger reversible capacity losses as compared with those of the fine nanorod electrode. The structural defects of the nanorods are favorable for the diffusion of Li ions into the CuO crystallites with the formation of the intercalated compound Li_xCuO.[22] The multipeaks are associated with differences in the lithium reaction process and can be attributed to the formation of the imperfection of highly organized nanotextured CuO lattice with polycrystalline structure, which facilitates the transport of lithium in surface defects and in bulk materials.

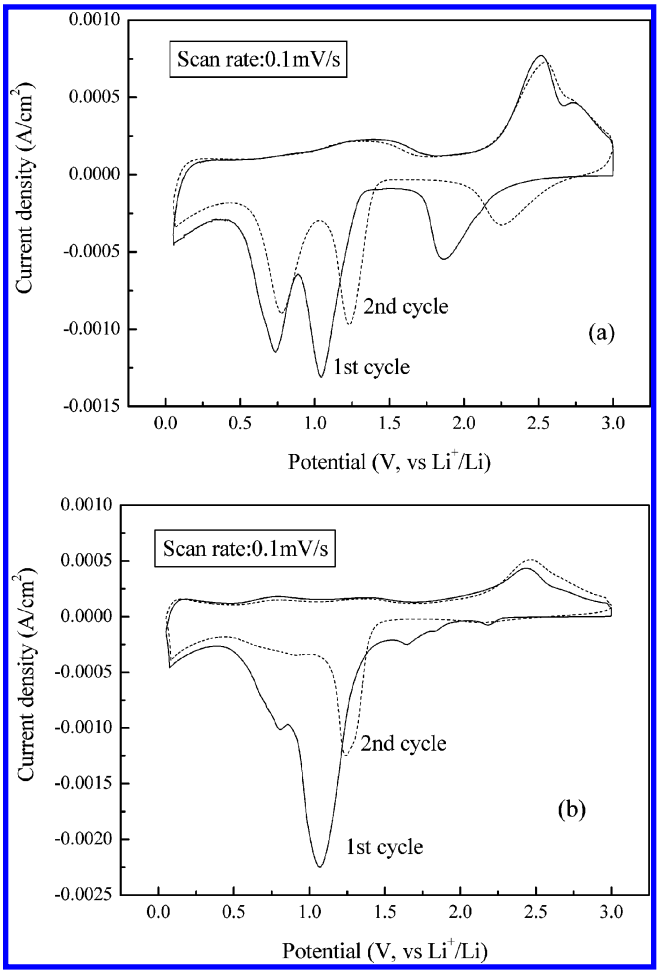

Figure 3. Cyclic voltammograms of as-prepared nanorods at room temperature (a) and 100 °C (b) at a scan rate of 0.1 mV/s.

The initial discharge−charge curves of the electrode made by the fine and bulk nanorods at the discharging and charging current density of 50 mA/g at room temperature are shown in Figure 4. There are three obvious sloping potential ranges (2.25−1.8, 1.25−1.0, and 1.0−0.02V vs Li^+/Li) for the lithium reaction with the fine CuO nanorods during the first discharge in accordance with three cathodic peaks in the above CVs. The first potential range (2.25−1.8 V) is narrowed and shifts slightly upward during the second discharge, accompanied by a decrease in the discharge capacity. The first and second discharge−charge curves of the bulk nanorods are similar to those of CuO spherical particles with 0.15 and 1 μm diameters as anode materials.[12] The wider (1.5−1.0 V) and narrower (1.0−0.02 V) potential ranges appear for lithium reaction with bulk CuO nanorods, but are different from that of the fine CuO nanorods. Moreover, the irreversible capacity loss of the bulk CuO nanorods after the first discharge increases, compared with that of the fine CuO nanorods. The change in potential range and irreversible capacity during the first and second discharges are consistent with the above observation in CVs. The interaction of nanorods with lithium ions takes place mostly at the surface rather than in the bulk as the crystal size decreases.[22] This means that the electrochemical reaction of lithium could be readily achieved in the fine CuO nanorods with polycrystalline structure because of their large specific surface area and numerous structural defects (grain boundary, oxygen vacancies, or the presence of OH^- groups[23]).

Cycle performance of the electrodes made by the fine and bulk nanorods at the discharging and charging current density

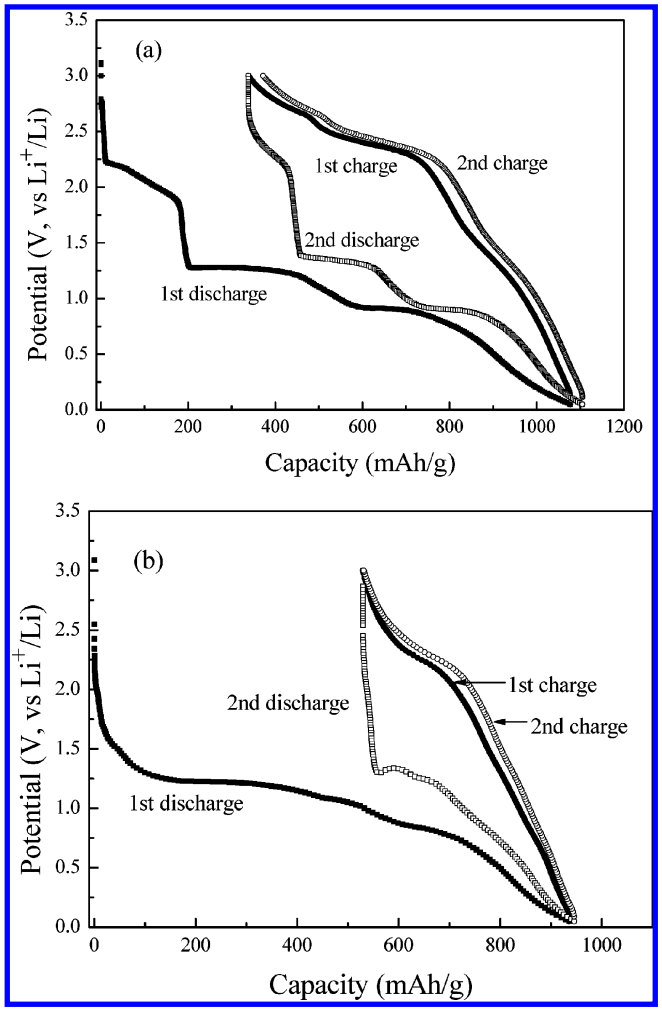

Figure 4. Discharge−charge curves of as-prepared nanorods at room temperature (a) and 100 °C (b) at discharging and charging current density of 50 mA/g at room temperature.

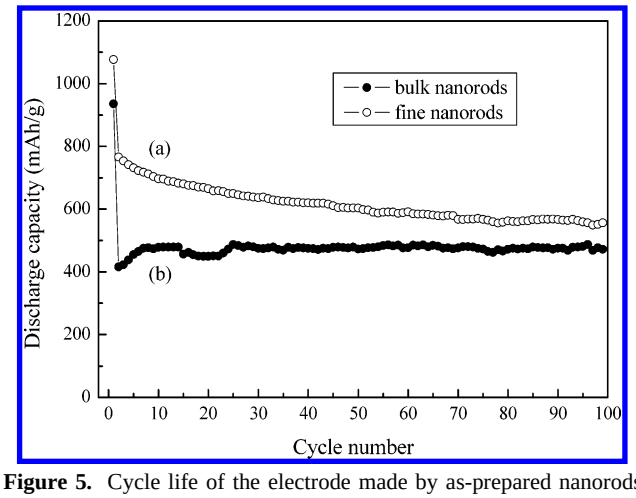

Figure 5. Cycle life of the electrode made by as-prepared nanorods at room temperature (a) and 100 °C (b) at discharging and charging current density of 50 mA/g at room temperature.

of 50 mA/g at room temperature is illustrated in Figure 5. The irreversible discharge capacity after the first cycle is due to the initial formation of lithium oxide.[24] The electrochemical reversible capacities of 766 and 416 mA h/g are achieved during the second discharge. Based on a maximum uptake of 2Li/CuO, the theoretical capacity of 674 mA h/g [25] is attained. The contribution of the reaction of lithium with carbon additive is at a magnitude of 60 mA h/g, and is thus not taken into account

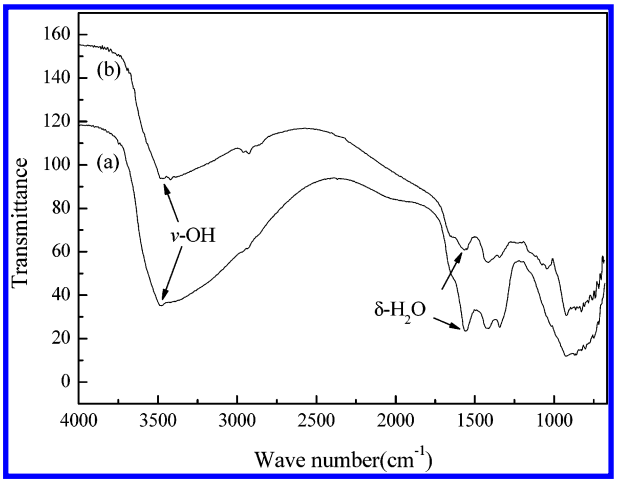

Figure 6. Infrared spectra of as-prepared nanorods at room temperature (a) and 100 °C (b).

for such high specific capacities.[26] The large excesses observed in capacity can also originate from the decomposition of the electrolyte and subsequent formation of an organic layer deposited on the surface of the particles that occurs in the low potential region for transition metal oxides.[26] On the other hand, the peak potential near 1.8 V (the actual peak potential depends on the scan rate) in the voltammetric curve is attributed to the presence of some residual OH^- groups in the active form of CuO.[25] From the infrared spectra of the nanorods prepared at room temperature and 100 °C (Figure 6), two stronger absorption bands at 1560 and 3470 cm^{-1} are observed, which are due to the bending vibration and stretching vibration, respectively, of adsorbed water. The stronger infrared absorption of the two bands for the fine nanorods obtained at room temperature suggests that this sample contains much more adsorbed water. The thermal gravimetric analysis (not shown) indicates a mass loss of about 1 wt % below 200 °C, which is completely due to the loss of the adsorbed water from the sample. Therefore, OH^- groups are mainly responsible for the higher discharge capacity of the CuO fine nanorods. The discharge capacity of the bulk nanorod electrode appeared to increase slightly during the first eight cycles due to crystal perfection, which usually proceeds with the activation process for electrochemical reaction of lithium. After 100 cycles, the CuO bulk nanorod electrode is able to keep its capacity at 470 mA h/g, while the electrochemical discharge capacity of the fine nanorod electrode decreases gradually to 550 mA h/g after 100 cycles.

Other researchers have identified that a change in the particle size of the precursor can strongly affect the capacity retention in transition metal oxides and $LiMn_2O_4$ for electrochemical reaction of lithium.[4,12,26,27] Novak[21] suggested that the discharge reaction involves intercalation of Li^+ ions into the CuO lattice according to $CuO + xLi^+ + xe^- \leftrightarrow Li_xCuO$. Grugeon[12] proposed a model involving the formation of metal nanograins during the first discharge and then the formation−decomposition of Li_2O concomitant with the reduction−oxidation of CuO on subsequent cycles. In general, the small particles are able to expand much more easily and can more easily accommodate the structural strains for the electrochemical reaction of lithium.[26] However, lithium interaction in a larger amount can trigger a phase transition and structure change. Therefore, the electrochemical Li-driven irreversible structural, morphological, and textural changes in the polycrystalline fine CuO nanorods could be more serious during cycling as compared to the single crystalline bulk CuO nanorods due to electrochemical reaction in a large amount. Therefore, the single crystalline structure of

copper oxide is more favorable for stable capacity of the electrochemical reaction of lithium. Nevertheless, its discharge capacity is lower, compared with that of the polycrystalline structure. A similar capacity decay in the electrochemical reaction of lithium was also reported in nanosized Cu_2O, CuO, and $LiMn_2O_4$, which is more rapid and serious than that in the corresponding microsized materials.[12,27]

IV. Conclusion

In summary, copper oxide nanorods of different crystalline structures and morphologies were synthesized successfully by a simple and efficient method in NaOH solution. The crystalline structure and morphology of the products are highly dependent upon the temperature of the hydrothermal treatment in the synthesis. The synthesis strategy could also be applied for the preparation of one-dimensional nanostructures of other transition metal oxides without any surfactant or template. The fine and polycrystalline CuO nanorods as anode materials for Li ion battery exhibit a high electrochemical capacity of 766 mA h/g, compared to 416 mA h/g for the single crystalline bulk nanorods due to their large surface area and numerous structural defects. However, the capacity retention of the fine CuO nanorods of polycrystals is not as good as that of bulk nanorods of a single crystal due to the Li-driven irreversible morphological and crystal changes during the cycles of the electrochemical reaction of lithium in a large amount.

Acknowledgment. This work is supported by 973 Programs (2002CB211800), the National Key Program for Basic Research (2001CCA05000), and the NSFC (90206043) of China. Financial support from the Australian Research Council (ARC) is also gratefully acknowledged, and H.Y.Z. is indebted to ARC for the QE II fellowship.

References and Notes

(1) Iijima, S.; Ichihashi, T. *Nature* **1993**, *363*, 603−605.
(2) Wen, J. G.; Lao, J. Y.; Wang, D. Z.; Kyaw, T. M.; Foo, Y. L.; Ren, Z. F. *Chem. Phys. Lett.* **2003**, *372*, 717−722.
(3) Yamamoto, K.; Kasuga, T.; Nogami, M. *Electrochem. Solid-State Lett.* **1999**, *2*, 595−596.
(4) Poizot, P.; Laruelle, S.; Grugeon, S.; Dupont, L.; Tarascon, J. M. *Nature* **2000**, *407*, 496−499.
(5) Poizot, P.; Hung, C. J.; Nikiforov, M. P.; Bohannan, E. W.; Switzer, J. A. *Electrochem. Solid-State Lett.* **2003**, *6*, C21−C25.
(6) Jia, D. Z.; Yu, J. Q.; Xia, X. *Chin. Sci. Bull.* **1998**, *43*, 172−174.
(7) Wu, H. Q.; Wei, X. W.; Shao, M. W.; Gu, J. S.; Qu, M. Z. *Chem. Phys. Lett.* **2002**, *364*, 152−156.
(8) Jiang, X. C.; Herricks, T.; Xia, Y. N. *Nano Lett.* **2002**, *2*, 1333−1338.
(9) Wang, W. Z.; Zhan, Y. J.; Wang, G. H. *Chem. Commun.* **2001**, 727−728.
(10) Sun, J. H.; Gong, Y. J.; Fan, W. H.; Wu, D.; Sun, Y. H. *Chem. J. Chin. Univ.* **2000**, *21*, 95−98.
(11) Tarascon, J. M.; Armand, M. *Nature* **2001**, *414*, 359−367.
(12) Grugeon, S.; Laruelle, S.; Herrera-Urbina, R.; Dupont, L.; Poizot, P.; Tarascona, J. M. *J. Electrochem. Soc.* **2002**, *148* (4), A285−A292.
(13) Joint Committee on Powder Diffraction Standards. Diffraction Data File No. 5-661; JCPDS International Center for Diffraction Data, Pennsylvania, 1991.
(14) Saito, Y.; Tani, Y.; Miyagawa, N.; Mitsushima, K.; Kasuya, A.; Nishina, Y. *Chem. Phys. Lett.* **1998**, *294*, 593−598.
(15) Kabalnov, A. J. *Dispersion Sci. Technol.* **2001**, *22* (1), 1−12.
(16) Kasuga, T.; Hiramatsu, M.; Hoson, A.; Sekino, T.; Niihara, K. *Langmuir* **1998**, *14*, 3160−3163.
(17) Wang, Y. Q.; Hu, G. Q.; Duan, X. F.; Sun, H. L.; Xue, Q. K. *Chem. Phys. Lett.* **2002**, *365*, 427−431.
(18) Yuan, Z. Y.; Colomer, J. F.; Su, B. L. *Chem. Phys. Lett.* **2002**, *363*, 362−366.
(19) Gao, X. P.; Zhu, H. Y.; Pan, G. L.; Ye, S. H.; Lan, Y.; Wu, F.; Song, D. Y. *J. Phys. Chem. B* **2004**, *108*, 2868−2872.
(20) Zhang, J.; Sun, L. D.; Yin, J. L.; Su, H. L.; Liao, C S.; Yan, C. H. *Chem. Mater.* **2002**, *14*, 4172−4177.
(21) Novak, P. *Electrochim. Acta* **1985**, *30*, 1687−1692.
(22) Kavan, L.; Rathousky, J.; Gratzel, M.; Shklover, V.; Zukal, A. *J. Phys. Chem. B* **2000**, *104*, 12012−12020.
(23) Podhajecky, P.; Zabransky, Z.; Novak, P.; Dobiasova, Z.; Cerny, R.; Valvoda, V. *Electrochim. Acta* **1990**, *35*, 245−249.
(24) Wu, G. T.; Wang, C. S.; Zhang, X. B.; Yang, H. S.; Qi, Z. F.; Li, W. Z. *J. Power Sources* **1998**, *75*, 175−179.
(25) Novak, P.; Klapste, B.; Podhajecky, P. *J. Power Sources* **1985**, *15*, 101−109.
(26) Larcher, D.; Masquelier, C.; Bonnin, D.; Chabre, Y.; Masson, V.; Leriche, J. B.; Tarascona, J. M. *J. Electrochem. Soc.* **2003**, *150* (1), A133−A139.
(27) Ye, S. H.; Lv, J. Y.; Gao, X. P.; Wu, F.; Song, D. Y. *Electrochim. Acta* **2004**, *49* (9−10), 1623−1628.